



Article

Tuning the Hydrophobicity and Lewis Acidity of UiO-66-NO₂ with Decanoic Acid as Modulator to Optimise Conversion of Glucose to 5-Hydroxymethylfurfural

Yongzhao Zhang ^{1,2}, Baiwen Zhao ¹, Satarupa Das ¹, Volkan Degirmenci ^{3,*}  and Richard I. Walton ^{1,*} ¹ Department of Chemistry, University of Warwick, Coventry CV4 7AL, UK² Ecology and Health Institute, Hangzhou Vocational & Technical College, Hangzhou 310018, China³ School of Engineering, University of Warwick, Coventry CV4 7AL, UK

* Correspondence: v.degirmenci@warwick.ac.uk (V.D.); r.i.walton@warwick.ac.uk (R.I.W.)

Abstract: Glucose conversion to 5-hydroxymethylfurfural (HMF) is important to the success of a biorefinery. Herein, metal–organic frameworks (MOFs) with the UiO-66 structure were synthesised with decanoic acid as the modulator and used as the catalyst to optimise HMF yield. PXRD, FTIR, and TGA/DSC techniques were applied to characterise the materials. The analysis results show that the materials assembled from the ligand 2-nitroterephthalic acid and hexameric Zr-oxo clusters contain decanoic acid chemically bound in the framework that influences porosity, Lewis acidity, and hydrophobicity. The materials exhibit excellent catalytic performance for HMF production from glucose in DMSO as solvent, attributed to their abundant defects and high hydrophobicity due to the addition of the decanoic acid modulator. Influences of catalyst dosages, reaction duration, and temperature were comprehensively investigated, leading to 98.1% conversion of glucose and 54.5% HMF yield under optimised reaction conditions. The catalytic conversion shows some deterioration after four cycles, yet the reaction selectivity displays no significant decline.

Keywords: 5-hydroxymethylfurfural; glucose; MOFs; UiO-66; modulator; decanoic acid



Citation: Zhang, Y.; Zhao, B.; Das, S.; Degirmenci, V.; Walton, R.I. Tuning the Hydrophobicity and Lewis Acidity of UiO-66-NO₂ with Decanoic Acid as Modulator to Optimise Conversion of Glucose to 5-Hydroxymethylfurfural. *Catalysts* **2022**, *12*, 1502. <https://doi.org/10.3390/catal12121502>

Academic Editors: Francis Verpoort and Somboon Chaemchuen

Received: 23 October 2022

Accepted: 18 November 2022

Published: 23 November 2022

Publisher's Note: MDPI stays neutral with regard to jurisdictional claims in published maps and institutional affiliations.



Copyright: © 2022 by the authors. Licensee MDPI, Basel, Switzerland. This article is an open access article distributed under the terms and conditions of the Creative Commons Attribution (CC BY) license (<https://creativecommons.org/licenses/by/4.0/>).

1. Introduction

The efficient conversion of cellulosic biomass, a cheap and abundant resource, can contribute to easing the dependence on fossil-derived hydrocarbons, and alleviate environmental issues and the energy crisis triggered by the excessive consumption of petroleum resources. Among various platform chemicals derived from biomass, 5-hydroxymethylfurfural (HMF) is considered as a promising intermediate compound to produce varieties of commodity chemicals [1–4]. However, the cost of HMF production is presently prohibitive economically. Therefore, great efforts have been made to reduce the production cost of HMF through innovative technology and catalyst design [5–11].

Highly selective production of HMF from fructose has been widely studied, and the highest HMF yield can reach up to 98% [12–14]. However, synthesising HMF from glucose, which is more abundant and has lower cost compared with fructose, is still challenging [15]. During the conversion, glucose is first isomerised into fructose, followed by the dehydration of fructose into HMF [16]. It is generally accepted that the isomerisation process is catalysed by Lewis acids and dehydration reaction with Brønsted acids. Therefore, designing and tuning catalysts to contain both Lewis and Brønsted acids for glucose conversion is crucial to improve selectivity towards the desired products. From this perspective, metal–organic frameworks (MOFs), in which metal or clusters are connected by ligands to form porous materials, constitute a promising class of catalysts for HMF production due to the ease of combining Lewis and Brønsted acidity within their structures [17]. Moreover, MOFs possess outstanding properties such as high surface area, tunable functional groups, and an atomic-level control over pore structure [18]. It is thus worth exploring the huge

potential in MOFs as catalysts for HMF production from glucose. Several MOFs have already been investigated for the production of HMF, e.g., MIL-101 [19], UiO-66 [20], Yb₆(BDC)₇(OH)₄(H₂O)₄ [21], NU-1000 [22], ZIF-8 [23], MIL-100 [24], MIL-53 [25], and MIL-88B [26]. Among these MOFs, the high stability and simple lab-scale synthesis of UiO-66 make it a desirable catalyst for HMF production [27].

Research has already been done to improve the catalytic properties of UiO-66 for glucose conversion. The catalytic properties of UiO-66 can be effectively tuned using different derivatives of benzene-1,4-dicarboxylates as ligands. Zhang et al. synthesised acid-base bi-functional UiO-66 type MOF catalysts with different ratios of monosodium 2-sulfoterephthalate and 2-aminoterephthalic acid, where the acidic and basic active sites worked synergistically for glucose conversion [28]. The catalytic properties of UiO-66 and its analogues (UiO-66-X, X = H, NH₂, and SO₃H) were investigated by Jue et al. and HMF yield of 28% was achieved under optimised reaction conditions [29]. Defect engineering is another important way to improve the catalytic properties of UiO-66. Fu et al. studied composition-activity relations for the UiO-66 catalysed dehydration of fructose into HMF [30]. The variation of the substituents on the NO₂/NH₂ functionalised solids showed an evident impact on the fructose dehydration, through affecting the number of missing linkers around Zr-oxo clusters, the hydrophobicity/hydrophilicity, and the Brønsted acidity. In the study by Oozeerally et al., UiO-66 was modified by partial linker substitution using sulfonyl derivatives, particle size modulation, and linker defects [31]. The effects of its crystallinity and functional groups on the glucose conversion in water were systematically explored. Other methods, such as using g-C₃N₄ as support doped with metal ions to improve the catalytic performance of UiO-66, have been reported [32–36].

In this work, two strategies have been applied to improve the synergy of Lewis and Brønsted acidity in UiO-66 as the catalyst for HMF production from glucose: (1) enhancement of Brønsted acidity by using 2-nitroterephthalate as the ligand via the electron-withdrawing effect of nitro groups [37]; (2) engineering of defects through addition of decanoic acid as modulator during sample synthesis to optimise the Lewis acidity. Moreover, the modulator present in the framework was also found to influence other properties of UiO-66, including surface area, pore volume, and hydrophobicity, further impacting its catalytic performance.

2. Results and Discussion

The crystallinity and phase purity of the UiO-66-NO₂-X materials were analysed by using PXRD, as shown in Figure 1. The PXRD patterns of all the samples are characterised by strongest peaks at angles of 7.4° and 8.5°, representing the crystal planes (111) and (200) that agree well with that expected for cubic UiO-66 with space group *Fm* $\bar{3}$ *m* [38]. Fitting the profile of the whole PXRD pattern indicates that all the samples possess the same UiO-66 framework topology. This also reveals that all the samples have almost the same unit cell size and that decanoic acid has no significant impact on it. However, differences occur in the patterns around the (111) reflection (the 2 θ ~7.4°), emphasised in Figure 2. As can be seen, there is a broad feature spanning a 2 θ range of 4–6° for the synthesised UiO-66-NO₂-X. This can be attributed to the *reo* phase, which is considered as UiO-66 with one-quarter of its clusters missing, according to the study conducted by Shearer et al. [39]. The presence of this broad peak therefore suggests that decanoic acid as modulator causes missing clusters, which leads to the formation of defects in the materials. To test this hypothesis, UiO-66-NO₂ was synthesised with formic acid as modulator under the same conditions. The broad diffraction feature mentioned above is not evident for this sample, indicating that formic acid has not such a significant influence on the orientation of clusters as decanoic acid, which may be due to its small steric effect. To investigate the effect of this defective structure further, the method developed by Feng et al. was applied to quantify the accessible Lewis acidic sites in MOFs, and the results are shown in Table 1 [40]. For the sample synthesised without modulator, the amount of Lewis acidic sites is too low to be detected. A significant enhancement of Lewis acidic sites is observed as amount of decanoic

acid is increased from 15 mmol to 25 mmol, and then decreases. In UiO-66-NO₂-25, the amount of Lewis acidic sites is 0.0061 mmol base per mg, which is about 15 times as high as that of formic acid (0.0004 mmol base per mg), suggesting a profound effect of decanoic acid on the number of Lewis acidic sites. It can be thus concluded that using decanoic acid as modulator is an effective way to enhance the Lewis acidity of UiO-66-NO₂.

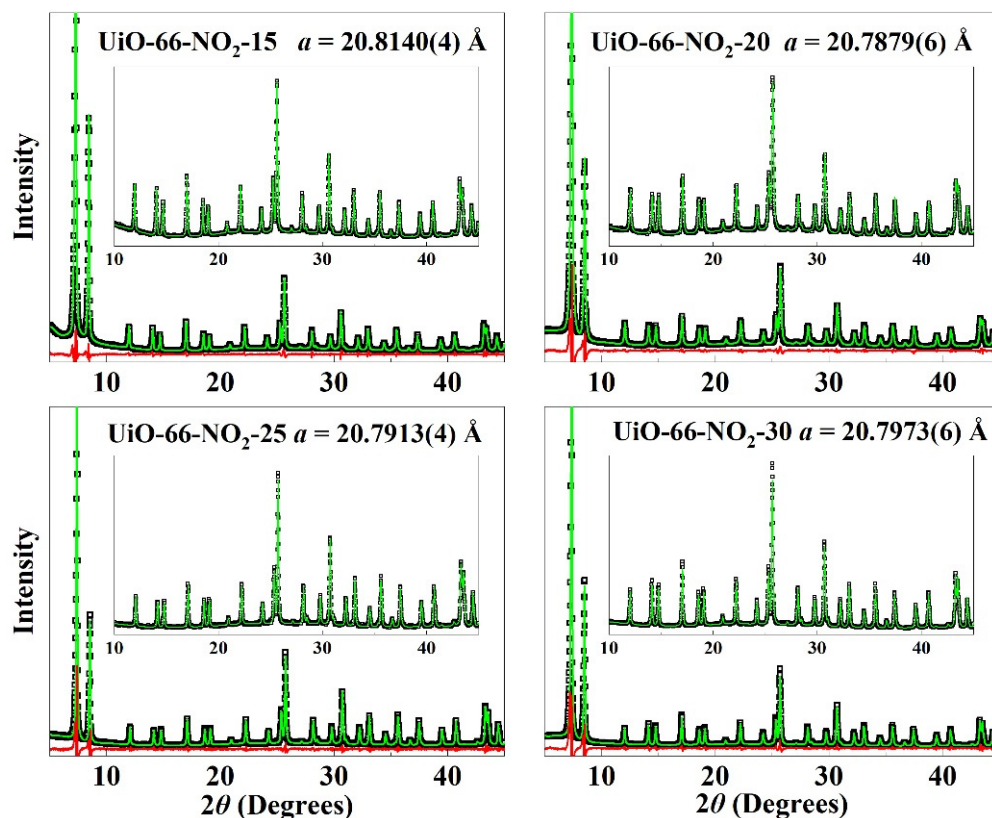


Figure 1. Profile fits to powder X-ray diffraction patterns of UiO-66-NO₂-X. The points are measured data, the green line is the final fit, and the red line the difference curve. Refined lattice parameters are provided on each panel. The refinement goodness-of-fit $wR = 5.61\%$, 9.40% , 11.60% , and 14.43% for $X = 15, 20, 25,$ and 30 in UiO-66-NO₂-X. The inset on each plot is an expanded region of the high angle region.

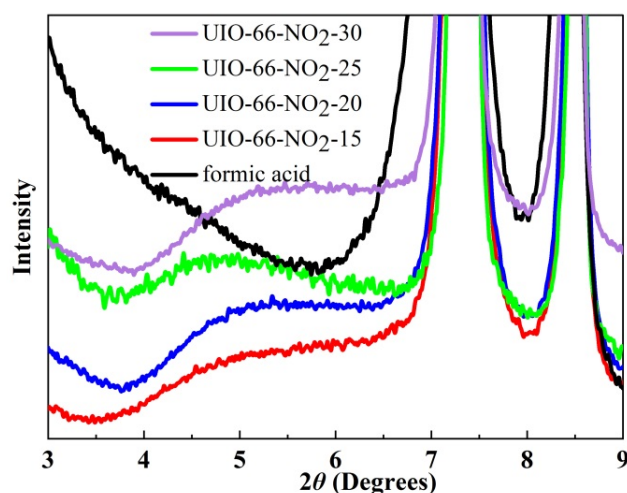


Figure 2. PXRD patterns of UiO-66-NO₂-X in the low-angle ($3\text{--}9^\circ$) region.

Table 1. Lewis acidic sites (mmol base per mg) in UiO-66-NO₂-X.

Entry	No Modulator	Formic Acid	UiO-66-NO ₂ -X			
			X = 15	X = 20	X = 25	X = 30
Lewis acidic sites	-	0.0004	-	0.0040	0.0061	-

- Not detected.

FTIR spectra are shown in Figure 3 and the detailed assignments of absorption bands are listed in Table 2. The peaks in the region of 1400–1600 cm⁻¹ are ascribed to the stretching of C=O, N=O and C=C in the organic ligands, and the anti-phase and in-phase bending of C-H in the benzene ring at 824 cm⁻¹ and 771 cm⁻¹ are also observed. The stretching of Zr-O in Zr-oxo clusters can be seen at 670 cm⁻¹. A band observed at 1655 cm⁻¹ is attributed to the stretching of carbonyl groups in DMF, revealing some DMF solvent remains in the pores of the framework. The bands at 2930 cm⁻¹ and 2850 cm⁻¹ attributed to methylene groups reveal that some decanoic acid is also present in UiO-66-NO₂-X. Given the evidence discussed below that shows it is chemically bound, this is likely present as decanoate, coordinated directly at the Zr centres. For other carboxylate modulators in UiO-66, this has proven to be the charge-balancing mechanism [39]. As shown in Figure 3, the intensity of methylene groups exhibits a non-monotonic trend with increasing decanoic acid loading. With the decanoic acid increasing from 15 to 30 mmol, the intensity increases first then decreases, inflecting at 25 mmol. A possible explanation could be that a proportion of channels in UiO-66-NO₂-X collapse when the amount of the modulator exceeds a certain amount, which inhibits the accumulation of the decanoic acid in MOFs. The result that UiO-66-NO₂-25 has the highest intensity of decanoic acid agrees with the Lewis acid quantification presented in Table 1. No peak is observed at 1770–1750 cm⁻¹, which is assigned to the carbonyl group in carboxylic acid, showing that no BDC-NO₂ and decanoic acid in free state exist in the framework, and this result is in agreement with the PXRD analysis results, which show no crystalline free acid.

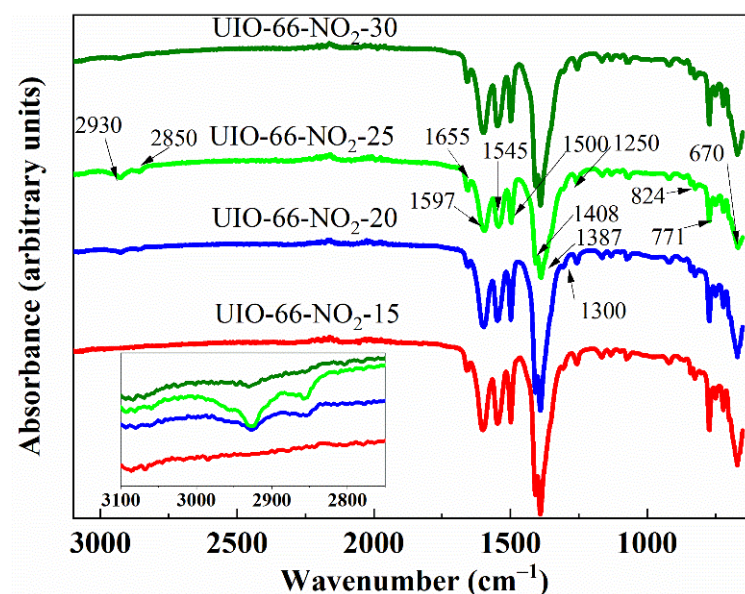
**Figure 3.** FTIR spectra of UiO-66-NO₂-X.

Table 2. Assignments of the FTIR peaks of UiO-66-NO₂-X.

Wave Number (cm ⁻¹)	Assignment
2930, 2850	CH ₂ asymmetric and symmetric stretching
1597, 1408	C=O asymmetric and symmetric stretching
1655	C=O stretching in DMF
1500	C=C stretching in phenyl moieties
1545, 1387	N=O asymmetric and symmetric stretching
1300	C-N stretching distinctive of BDC-NO ₂
1250	C-H stretching
824, 771	C-H anti-phase and in-phase bending
670	Zr-O stretching

Nitrogen adsorption–desorption isotherms of all samples were measured at 77 K to elucidate their textural properties. As illustrated in Figure 4, the isotherms of UiO-66-NO₂-X show Type I patterns. A steep increase of nitrogen adsorption at P/P_0 of 0–0.1 is observed, evidencing a narrow micropore size distribution in UiO-66-NO₂-X. The textural properties of all samples are shown in Table 3. When no modulator is added, the sample has poor porous properties, with BET surface area and pore volume are 367.52 m²/g and 0.136 cm³/g, respectively. Introduction of decanoic acid as modulator can improve the porous properties of UiO-66-NO₂ greatly due to the formation of defects, and UiO-66-NO₂-X exhibit high surface area and pore volume. The effect of modulators has also been reported in literature [41], where the surface area of UiO-66 improved from 439 m²/g to 1410 m²/g with increasing concentration of modulator. The amount of decanoic acid as modulator has some degree of influence on the textural properties of UiO-66-NO₂-X but this influence becomes insignificant when the amount of decanoic acid exceeds 25 mmol. The effect of decanoic acid could be explained through two aspects: (1) facilitating the formation of defects to improve porous properties; (2) occupation of decanoic acid to fill the void space and lower porosity. Under the collective influence of these two effects, the UiO-66-NO₂-20 shows a relatively lower surface area and pore volume compared with other samples. As the amount of decanoic acid is increased from 15 mmol to 20 mmol, the occupation effect becomes significant, and the surface area and pore volume deteriorate. With a further increase in amount of decanoic acid, more defects in MOFs are formed, and the surface area and pore volume improve. The occupation of decanoic acid is suggested by the variation of porous properties of UiO-66-NO₂-25 after soaking treatment in HCl-DMF mixture for the partial removal of decanoic acid, whereupon the surface area and pore volume increase by nearly 11% and 8%, respectively. Further examination of the existence of decanoic acid molecules and their existing states are investigated and discussed below.

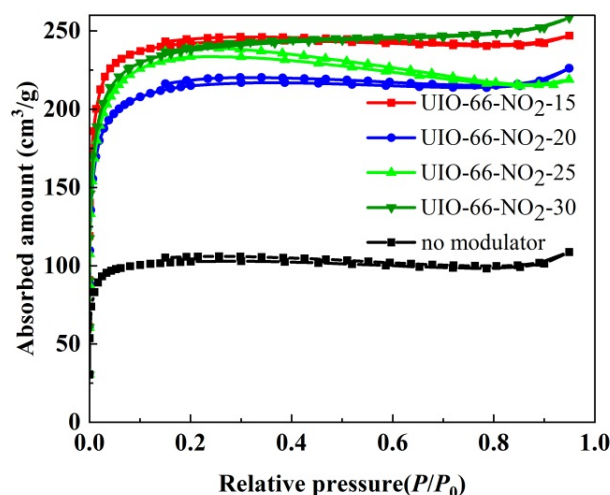
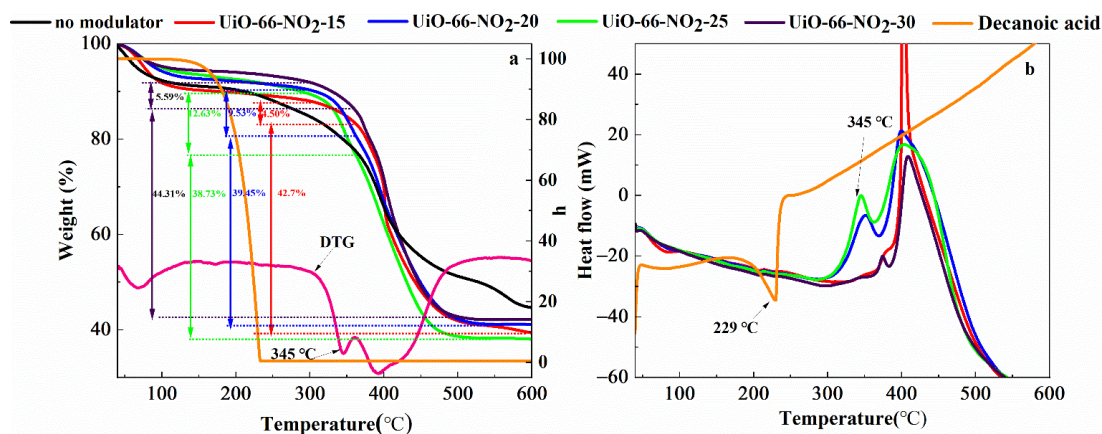
**Figure 4.** Nitrogen adsorption–desorption isotherms of UiO-66-NO₂-X.

Table 3. Analysis of nitrogen adsorption isotherms of UiO-66-NO₂-X.

Entry	UiO-66-NO ₂ -X					
	No Modulator	X = 15	X = 20	X = 25	X = 30	X = 25 *
BET surface area(m ² /g)	367.52	871.96	772.42	842.13	853.88	935.62
t-plot micropore volume (cm ³ /g)	0.136	0.318	0.254	0.274	0.281	0.296

* soaking treatment in HCl-DMF.

Simultaneous TGA-DSC was applied to characterise the thermal stability and chemical composition of UiO-66-NO₂-X. Figure 5a shows the mass loss curves. The differential scanning calorimetry (DSC) curves are shown in Figure 5b. The differential TG (DTG) curves of UiO-66-NO₂-X all show a similar trend, and only the curve of UiO-66-NO₂-25 is given in Figure 5a to highlight the distinctive mass loss events. As temperature is increased from 50 to 150 °C, an approximate 10% mass loss is observed due to the removal of physisorbed water and solvent. A slight loss (about 2%) is attributed to the removal of DMF solvent or the dehydroxylation of the Zr-oxo cluster with the temperature increase from 150 to 300 °C. With temperature increase further up to 600 °C, there exists a continuous mass loss with no clear discontinuities. It is therefore not possible to separate the combustion of linker and combustion of modulator and to assign unambiguously the relative amount of linker, especially bearing in mind variable presence of defects between each sample. Subsequently, ZrO₂ is formed, with a remaining weight of 40% approximately, and no further significant weight loss observed above 600 °C. The final remaining mass of UiO-66-NO₂-25 is lower than that of other samples which implies a higher decanoic acid percentage. No significant framework decomposition is found below 300 °C, suggesting that UiO-66-NO₂-X materials show good thermal stability. In Figure 5b, no significant endothermic peak appears at 229 °C for UiO-66-NO₂-X, at which is the maximum decomposition rate of decanoic acid, showing that no detectable free decanoic acid exists in the MOFs. The maximum decomposition rate of the MOFs prepared with decanoic acid as modulator occurs at 345 °C, and an exothermic peak can be found at the same temperature in Figure 5b, indicating that decanoic acid is combusted with release of heat when it decomposes from the framework. In consideration of the proof from FTIR analysis that methylene groups from decanoic acid do exist in the samples, it can be concluded that the remaining decanoic acid in UiO-66-NO₂-X is chemically bound in the framework, making its decomposition temperature much higher than that of pure decanoic acid. To test the possibility that decanoic acid is present only in small amounts, TGA-MS analysis was carried out, but this showed no signal related to decanoic acid, validating that none exists in a free state in the UiO-66-NO₂-X samples.

**Figure 5.** (a) TGA curves and (b) DSC curves of UiO-66-NO₂-X. In (a) the DTG curve of UiO-66-NO₂-20 is shown in pink.

The catalysis results are shown in Figure 6, in which results from oUiO-66-NO₂ synthesised with other modulators (formic acid, butyric acid, benzoic acid, and trifluoroacetic acid) are also given. For fructose dehydration into HMF, conversion of fructose and HMF yield are 80% and 48%, respectively, when no catalyst is added. The reason is that mercaptan is formed for the decomposition of DMSO at high temperature and this can be oxidised into sulfonic acid, an efficient catalyst for fructose dehydration. UiO-66-NO₂ synthesised with different modulators manifests lower catalytic properties, compared with the one prepared without modulator. It is generally accepted that the main source of Brønsted acidity in UiO-66 is μ_3 -OH in the hexameric clusters and this is decisive to the successful conversion of fructose to HMF [37]. As modulators are added during the synthesis of UiO-66, some Brønsted acid sites are lost owing to the missing clusters, leading to the decline of catalytic performance. Surprisingly, this decline is not seen when decanoic acid is used as the modulator, and in fact conversion, yield, and selectivity are increased, revealing that decanoic acid might possess some distinctive effects on conversion of fructose.

For HMF production from glucose, conversion of glucose and HMF yield improve greatly after catalyst addition compared to when no catalyst is used. Among all the samples, UiO-66-NO₂-25 exhibits the best catalytic properties, with 89.5% conversion of glucose and 44.8% HMF yield, indicating that UiO-66-NO₂-25 possessed the best combination of Lewis and Brønsted acid sites, facilitating glucose isomerisation and fructose dehydration. According to molecule size calculation, the chain length of decanoic acid is about 13 Å, which is much larger than that of BDC-NO₂ (approximately 6 Å). The coordination of decanoic acid to Zr⁴⁺ might hinder the orientation of Zr-oxo clusters at nearby positions, creating Lewis acidic sites. Moreover, decanoic acid in the framework is likely to increase the hydrophobicity of MOFs, preventing Lewis acidic sites being deactivated by water and increasing the diffusion of water out of the catalyst in favour of glucose conversion into desired product. The hydrophobicity of UiO-66-NO₂-X is seen qualitatively upon dispersing in water, which is shown in Figure 7. It can be seen that UiO-66-NO₂-25 floats on the water surface, evidencing a high hydrophobicity. We conclude that it is the synergistic effect of Lewis and Brønsted acidity and hydrophobicity that makes UiO-66-NO₂-25 an efficient catalyst for HMF production.

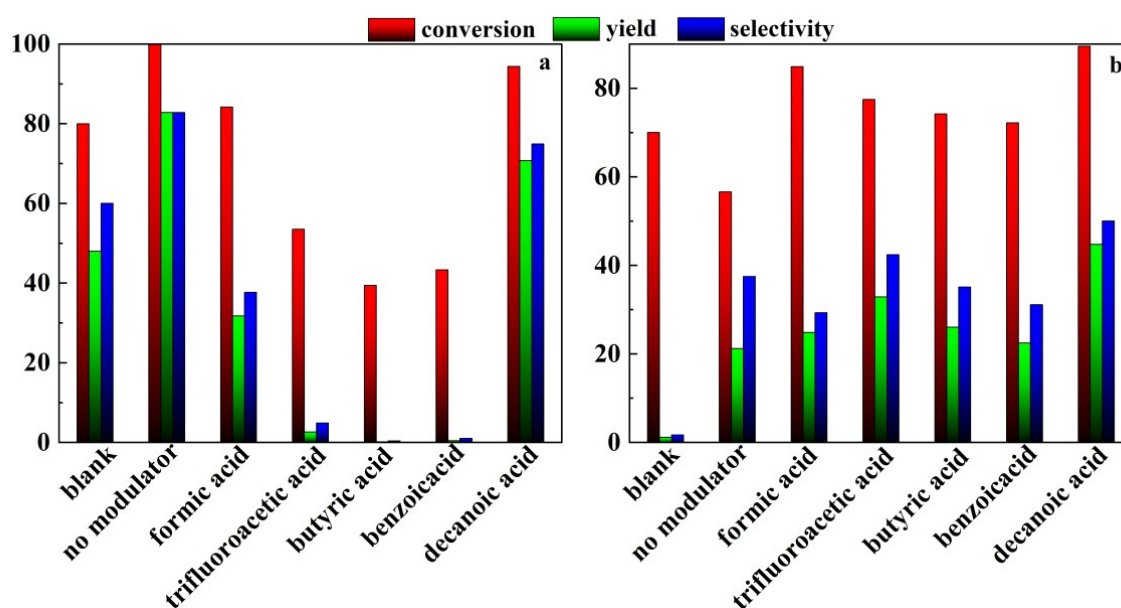


Figure 6. Effect of modulator type on HMF production from (a) fructose and (b) glucose.

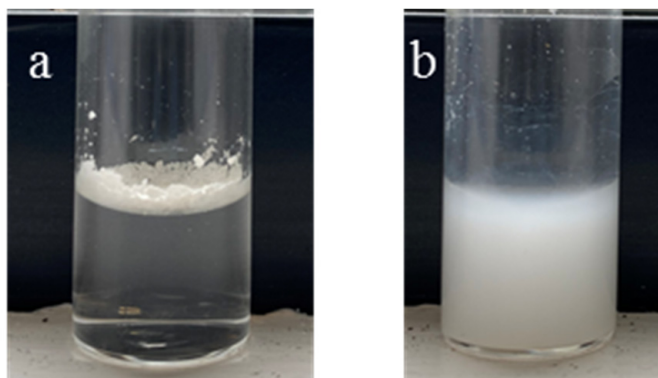


Figure 7. (a) Dispersion of as-made UiO-66-NO₂-25 in water and (b) after soaking.

To further explore the role of decanoic acid remaining in the samples, the catalytic properties of UiO-66-NO₂-25 after treatment by soaking in HCl-DMF mixture (0.6 or 0.8 mL HCl + 20 mL DMF) for glucose conversion were investigated. As shown in Figure 8, the intensity of methylene groups seen in the FTIR spectrum decreases after soaking, indicating partial removal of decanoic acid from the sample. This can also be validated from the enhancement of surface area and pore volume after soaking shown in Table 3. The decline of catalytic properties after soaking for UiO-66-NO₂-25 is shown in Figure 9. Conversion of glucose and HMF yield drop from 89.5% to 82.8%, 44.5% to 31.3%, respectively, and this decrease is more significant for fructose conversion. It can thus be concluded that decanoic acid remaining in the framework plays an important role in increasing the catalytic performance for HMF production.

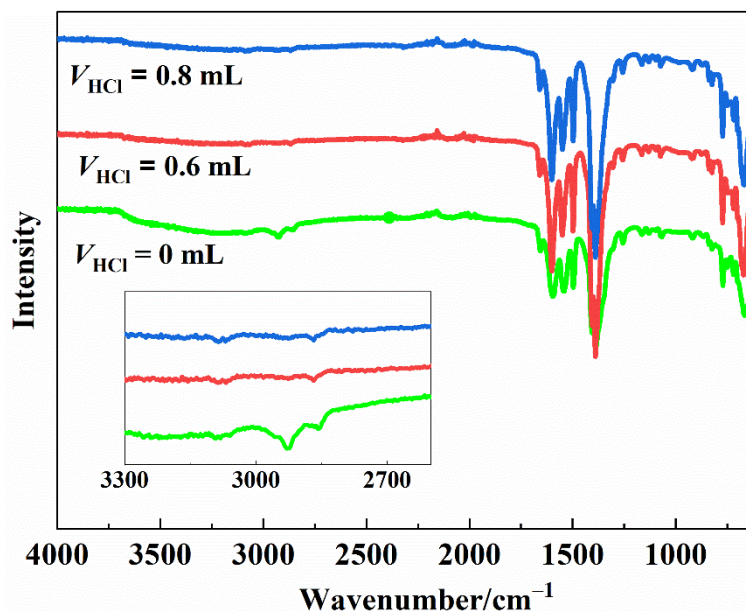


Figure 8. FTIR spectra of UiO-66-NO₂-25 after soaking in HCl-DMF mixture.

UiO-66-NO₂-X prepared with different amounts of decanoic acid for glucose conversion were also analysed and the reaction results are shown in Figure 10. Conversion of glucose and HMF yield reach the maximum value when the amount of decanoic acid is 20 and 25 mmol, then decreases upon further addition of the modulator. As mentioned above, decanoic acid improves the Lewis acidity and hydrophobicity of MOFs, which favour glucose conversion. Consequently, an enhancement of catalytic performance of UiO-66-NO₂-X is observed as the amount of modulator increases. However, presence of

further amounts of decanoic acid molecules and imbalance of Lewis and Brønsted acids have a negative impact on glucose conversion.

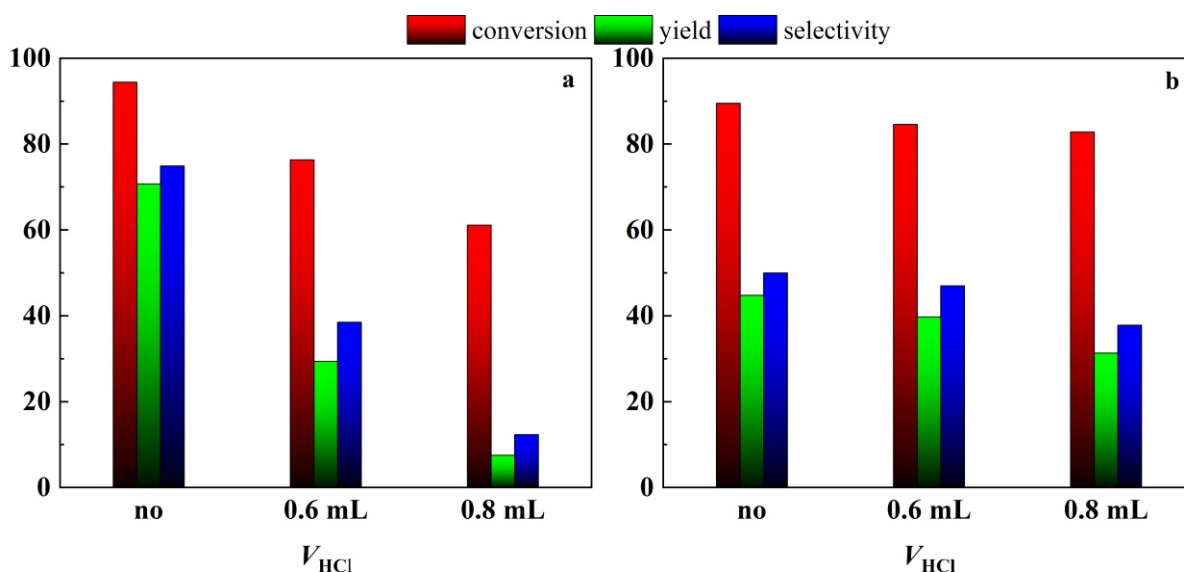


Figure 9. Decline of catalytic properties of UIO-66-NO₂-25 for HMF production from (a) fructose and (b) glucose after soaking.

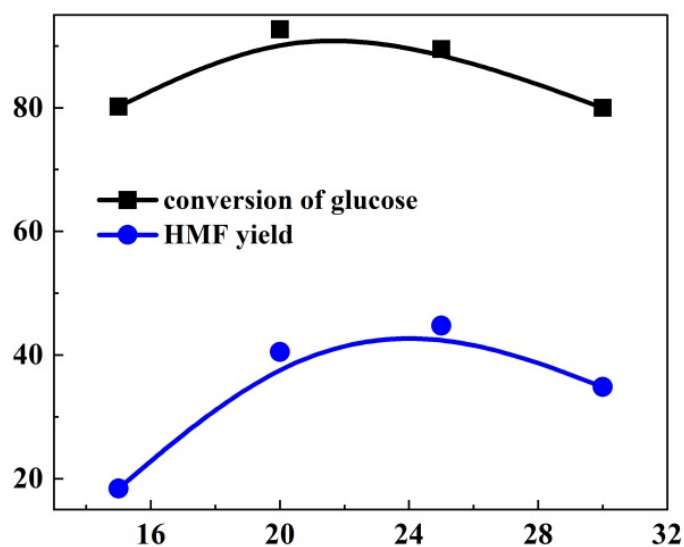


Figure 10. Effect of amount of decanoic acid on HMF production from glucose.

Figure 11a shows the effect of catalyst dosages on the HMF production from glucose. When 5 mg of catalyst is added, conversion of glucose and HMF yield are 88.8% and 33.9%, respectively, after 4 h, exhibiting the effectiveness of this catalyst. Conversion of glucose and HMF yield improve to 98.1% and 54.5% as the catalyst dosage is increased up to 15 mg. Further increase of catalyst dosage seemingly has no significant promotion on HMF formation, indicating that higher catalyst dosage might give rise to side reactions. Therefore, the catalyst dosage was fixed at 15 mg for subsequent reactions to obtain optimum HMF yield.

As the glucose isomerisation and fructose dehydration are endothermic, temperature has an obvious influence on HMF yield. In order to optimise HMF yield, the process of glucose conversion was monitored as a function of time at three temperatures, which is shown in Figure 11b. A maximum 54.5% HMF yield is achieved at 140 °C after 4 h. Higher temperature (150 °C) can cause HMF decomposition after a longer time, leading to the

decline of HMF yield. Moreover, HMF formation proceeds slowly at 130 °C, and HMF yield is 48.0% after 6 h. Furthermore, it can be found that further prolonging of reaction time over optimised conditions decreases HMF yield, which may be due to the decomposition of HMF. The optimal reaction conditions are as follows: 15 mg of catalyst and 27.5 mg glucose at 140 °C for 4 h in 1.25 mL DMSO.

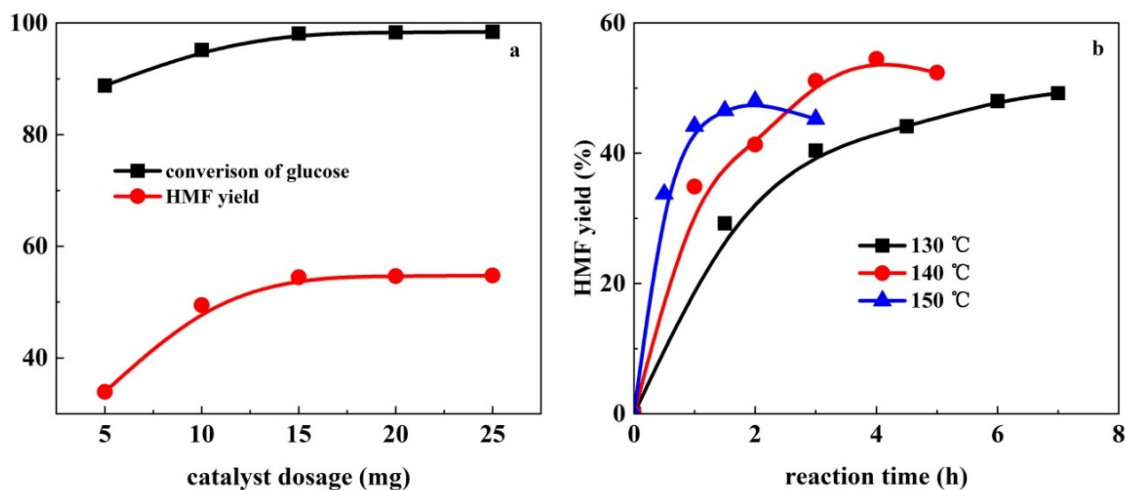


Figure 11. (a) Effect of catalyst dosages on glucose conversion and HMF yield; (b) Effect of reaction time under different temperatures on HMF production from glucose.

The recyclability of catalyst is important from the perspective of sustainable chemistry and economic cost. Recycling experiments were carried out to investigate the reusability of catalyst with the reaction results shown in Figure 12. After four cycles, glucose conversion declines from about 90% to 50%, and HMF yield from 50% to 20%. The reason for this decline is likely due to the accumulation of humins on the exterior and interior surface of the catalyst, deactivating some active sites and hindering the diffusion of glucose. However, the catalytic selectivity does not show a significant deterioration, suggesting the active sites in the samples maintain their catalytic properties for glucose conversion into HMF instead of other side products.

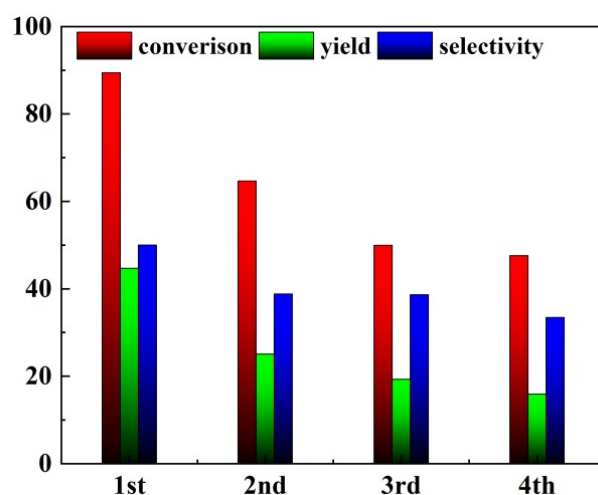


Figure 12. Recyclability test of UiO-66-NO₂-25 for HMF production from glucose showing percentage conversion, yield and selectivity.

To investigate the influence of solvent, the glucose conversion was studied in various solvents and mixed solvents, and the results are summarised in Table 4. This shows always a lower HMF yield compared with that in DMSO. As 10% water is added in DMSO, HMF

yield declines from 44.8% to 24.3%. HMF yield does not show improvements when MIBK is used to extract HMF from water in a biphasic system. These results suggest the deactivation effect of water on UiO-66-NO₂-25. HMF yield in DMF is 4.8%, meaning that DMF can deteriorate the catalytic performance significantly, possibly due to its basic characteristics.

Table 4. Solvent effect on glucose conversion.

Entry	Solvent	θ (°C)	Time (h)	Glucose Conversion (%)	HMF Yield (%)	Selectivity (%)
1	Water		3	55.2	5.6	10.1
2	DMF		3	88.3	4.8	5.4
3	Water/MIBK($v/v = 1/2$)		4	57.8	4.6	8.0
4	Water/DMSO($v/v = 1/9$)	140	4	72.6	24.3	33.5
5	Water/DMF($v/v = 1/9$)		4	100	0.1	0.1
6	Water/acetone($v/v = 1/9$)		4	-	1.4	-
7	Water/2-propanol($v/v = 1/9$)		4	-	3.9	-

- Not analysed.

Table 5 summarises some heterogeneous catalysts previously reported in the literature for glucose conversion to HMF. It can be seen that the UiO-66-NO₂ synthesised with decanoic acid as modulator exhibits desirable catalytic properties with high conversion of glucose and HMF yield in DMSO. Only a few studies have reported higher HMF yield [32,42], but these other high performing catalysts are composite materials with complex synthesis procedures. UiO-66-NO₂-25 synthesised in our work is a desirable catalyst for glucose conversion, which has a low synthesis cost, high catalytic performance, and outstanding porous properties. For comparison, the sulfonated MOF MIL-101(Cr) shows very poor performance in DMSO [43]. Some materials manifest much better catalytic performance in aqueous systems compared with the catalyst in our work, yet they are generally different classes of materials, inorganic frameworks or mesoporous silica [44–46]. An exception is phosphate-modified NU-1000, where a zirconium-based MOF is modified by post-synthetic treatment with phosphoric acid [22]. This gives an outstanding catalytic performance, but the mass fraction of glucose is as low as 0.018%, which is much lower than that applied in our work (2%). However, for this material HMF yield declines greatly to about 20%, when the glucose concentration increases to 1.8%, and recyclability was not investigated.

Table 5. Reported glucose conversion to HMF catalysed by heterogeneous catalysts.

Catalyst	θ (°C)	Time (min)	Solvent	Glucose Conversion (%)	HMF Yield (%)	Ref
UiO-66-NO ₂ -25	140	240	DMSO	98.1	54.5	This work
MIL-88(Fe,Sc)	140	180	DMSO	71.0	25.1	[26]
MIL-101(Cr)-SO ₃ H	120	120	DMSO	not given	7	[43]
MIL-101(Sn,Cr)	140	60	DMSO	85.7	22.6	[19]
UiO-66-NH ₂ -SO ₃ H	140	600	DMSO	not given	45.2	[28]
UiO-66-NH ₂ -SO ₃ H@g-C ₃ N ₄	120	360	Isopropanol/DMSO	92	55	[32]
UiO-66-SO ₃ H	140	180	Water	36	8	[31]
MSDBC(50)-naphtha(50)-UiO-66	120	180	Water	33	7	
SnPCP@MnO ₂ -PDA	150	180	DMSO	90	55.8	[42]
P-3Ti/SBA-15	160	180	Water/mTHF	98	71	[44]
Sn modified SAPO-34	150	90	NaCl/Water/THF	98.5	64.4	[45]
Phosphate-modified NU-1000	140	420	Water/ 2-propanol	>99	64	[22]
Sn-Beta, HCl	180	70	NaCl/Water/THF	79	56.9	[46]

3. Materials and Methods

3.1. Chemicals and Reagents

Zirconium tetrachloride ($ZrCl_4$, 99.5%, Sigma-Aldrich, Gillingham, UK), 2-nitroterephthalic acid (BDC- NO_2 , 99%, Sigma-Aldrich, Gillingham, UK), formic acid (99%, Sigma-Aldrich, Gillingham, UK), butyric acid (99%, Acros Organics, Geel, Belgium), trifluoroacetic acid (99%, VWR, Poole, UK), benzoic acid (99.5%, Alfar Aesar, Heysham, UK), decanoic acid (99%, Alfar Aesar, Heysham, UK), *N,N*-dimethylformamide (DMF, 99%, Fisher Scientific, Loughborough, UK), glucose (99%, Millipore, Watford, UK), fructose (99%, Alfar Aesar, Heysham, UK), dimethyl sulfoxide (DMSO, 99.5%, Sigma-Aldrich, Gillingham, UK), hydrochloric acid (HCl, 37%, VWR, Poole, UK), methyl isobutyl ketone (MIBK, 99%, Sigma-Aldrich, Gillingham, UK), acetone (99.5%, Sigma-Aldrich, Gillingham, UK), and 2-propanol (99.5%, Sigma-Aldrich, Gillingham, UK). All chemicals were used as received.

3.2. Preparation of UiO-66- NO_2

UiO-66- NO_2 was synthesised as follows: 1 mmol $ZrCl_4$, 0.5 mmol BDC- NO_2 , and specified moles of decanoic acid were dissolved completely in 18 mL DMF. The mixture was then transferred into a PTFE-lined autoclave and heated at 120 °C for 24 h. The resulting white solid was filtered, washed with DMF twice, and soaked in DMF at 90 °C for 12 h. Finally, the solid was washed with DMF and acetone twice for each solvent, and the obtained UiO-66- NO_2 was dried at 150 °C overnight. Samples of UiO-66- NO_2 with different amounts of decanoic acid are labeled as UiO-66- NO_2 -X, where X represents the number of moles (mmol) of added decanoic acid. Four samples were synthesised with X of 15, 20, 25, and 30. To investigate the effect of decanoic acid, the sample with no modulator added was also prepared for comparison.

3.3. Materials Characterisation

The physical and chemical properties of the as-synthesised UiO-66- NO_2 -X were characterised by various techniques. Powder X-ray diffraction (PXRD) analysis was carried out using a Panalytical Empyrean diffractometer (Malvern Panalytical, Malvern, UK) operating with Cu $K\alpha_{1/2}$ radiation to investigate the crystal structure of UiO-66- NO_2 -X. The software GSAS-II was used to perform profile fitting of the diffraction patterns using the Pawley method [47]. Surface area, pore volume, and pore diameter distribution were analysed with N_2 adsorption–desorption experiment at 77 K using a Micromeritics ASAP 2020 apparatus (Micromeritics, Tewkesbury, UK). A Nicolet Nexus 470 Fourier transform infrared (FTIR) spectrometer (Thermo Fisher Scientific, Waltham, MA, USA.) was used to identify the functional groups in the samples. Thermogravimetric analysis (TGA) and differential scanning calorimetry (DSC) were conducted using a Mettler Toledo TGA/DSC instrument (Mettler-Toledo, Leicester, UK) under an air flow up to 600 °C with a heating rate of 10 °C/min to investigate thermal stability of the samples.

3.4. Catalytic Reactions and Analysis Technique

The catalytic reactions for HMF production from glucose were performed in an oil bath. Glucose (27.5 mg) was added to a 4 mL thick-walled glass vial (Kinesis, Eaton Socon, UK) containing 1.25 mL DMSO, and the mixture was stirred continuously during heating with a magnetic bar to ensure homogeneous conditions. After the chosen reaction time, the mixture was diluted with deionised water and analysed by using high performance liquid chromatography (HPLC).

Glucose and HMF were quantified using an HPLC instrument (Shimadzu, Milton Keynes, UK) equipped with an Aminex HPX-87H 300 mm × 7.8 mm column (Bio-Rad Laboratories, Hercules, CA, USA), UV, and ELSD detectors. The specific parameters are as follows: column temperature of 50 °C, water as the mobile phase at flow rate of 0.4 mL/min, UV detection wavelength at 284 nm, and injection volume of 10 μ L. Conversion of glucose and HMF yield were obtained based on standard calibration curves that were fitted from

known concentrations of glucose and HMF standard solutions. Conversion of glucose, HMF yield, and reaction selectivity towards HMF are calculated as follows:

$$\text{Conversion}_{\text{glucose}}(\text{mol}\%) = \frac{\text{moles of glucose reacted}}{\text{moles of starting glucose}} \times 100\% \quad (1)$$

$$\text{Yield}_{\text{HMF}}(\text{mol}\%) = \frac{\text{moles of HMF produced}}{\text{moles of starting glucose}} \times 100\% \quad (2)$$

$$\text{Selectivity}_{\text{HMF}}(\text{mol}\%) = \frac{\text{HMF yield}}{\text{glucose conversion}} \times 100\% \quad (3)$$

3.5. Quantification of Accessible Lewis Acidic Sites

The accessible Lewis acidic sites were quantified as follows according to literature [40]: about 20 mg of MOFs was treated with 0.5 mL pivalonitrile in toluene for 24 h at room temperature. The resultant solid was centrifuged and washed with toluene thoroughly to remove excess pivalonitrile, then washed with acetone to remove toluene. The final material was dried and digested in $\text{NH}_4\text{F}/\text{D}_2\text{O}$. The mixture was analysed by ^1H NMR, in which 1, 4-dioxane was used as an internal standard. Then the quantity of pivalonitrile ($m_{\text{pivalonitrile}}$) in the sample was calculated as follows:

$$m_{\text{pivalonitrile}} = \frac{I_{\text{pivalonitrile}}}{I_{\text{standard}}} \frac{N_{\text{standard}}}{N_{\text{pivalonitrile}}} \frac{M_{\text{pivalonitrile}}}{M_{\text{standard}}} m_{\text{standard}} \quad (4)$$

where $I_{\text{pivalonitrile}}$ is the integral of the pivalonitrile peak, $N_{\text{pivalonitrile}}$ is the number of protons corresponding to the pivalonitrile, $M_{\text{pivalonitrile}}$ is the molar mass of pivalonitrile, and m_{standard} is the known mass of the standard in the sample.

3.6. Recyclability of Catalysts

For recyclability experiments, the catalysts were recovered from the reaction mixture by centrifugation after the completion of the reaction. The recovered catalysts were washed thoroughly with water and acetone, respectively, followed by drying at 150 °C. Subsequently, the dried catalysts were used for four consecutive cycles. To eliminate the influence of a little amount of catalyst loss on recyclability experiments, the first run was duplicated for six times, ensuring that the amount of the recovered catalyst is enough for the subsequent reactions.

4. Conclusions

UiO-66 MOFs were prepared with 2-nitroterephthalate as linker and decanoic acid as modulator. The decanoic acid present in the MOF structure is chemically bound and influences the porous and catalytic properties, including surface area and pore volume, Lewis acidity, and hydrophobicity. The samples exhibit efficient catalytic performance for conversion of glucose to HMF. Under optimised reaction conditions, conversion of glucose and HMF yield can reach up to 98.1% and 54.5%, respectively. During the process of glucose conversion, humins formed as the side product can deteriorate the catalytic conversion of samples, yet the reaction selectivity towards HMF is almost maintained. Future work must consider further quantification of acidity, both Lewis and Brønsted, to understand more fully the mechanism of catalysis.

Author Contributions: Conceptualization, Y.Z., V.D. and R.I.W.; formal analysis, Y.Z., B.Z. and S.D.; writing—original draft preparation, Y.Z.; writing—review and editing, Y.Z. and R.I.W.; supervision, V.D. and R.I.W. All authors have read and agreed to the published version of the manuscript.

Funding: This research was financially supported by Hangzhou Science and Technology Bureau [20170432B25].

Data Availability Statement: Data are available from the authors on request.

Acknowledgments: We are grateful to China Scholar Council (CSC) and University of Warwick's Research Technology Platforms for the provision of some of equipment used in this work.

Conflicts of Interest: The authors declare no conflict of interest. The sponsors had no role in the design, execution, interpretation, or writing of the study.

References

1. van Putten, R.J.; van der Waal, J.C.; de Jong, E.D.; Rasrendra, C.B.; Heeres, H.J.; de Vries, J.G. Hydroxymethylfurfural, a versatile platform chemical made from renewable resources. *Chem. Rev.* **2013**, *113*, 1499–1597. [\[CrossRef\]](#)
2. Fan, W.; Verrier, C.; Queneau, Y.; Popowycz, F. 5-Hydroxymethylfurfural (HMF) in organic synthesis: A review of its recent applications towards fine chemicals. *Curr. Org. Synth.* **2019**, *16*, 583–614. [\[CrossRef\]](#) [\[PubMed\]](#)
3. Yue, X.; Queneau, Y. 5-Hydroxymethylfurfural and Furfural Chemistry Toward Biobased Surfactants. *ChemSusChem* **2022**, *15*, e202102660. [\[CrossRef\]](#)
4. Wang, Y.; Wang, H.; Kong, X.; Zhu, Y. Catalytic Conversion of 5-Hydroxymethylfurfural to High-Value Derivatives by Selective Activation of C–O, C=O, and C=C Bonds. *ChemSusChem* **2022**, *15*, e202200421. [\[CrossRef\]](#)
5. Rosenfeld, C.; Konnerth, J.; Sailer-Kronlachner, W.; Solt, P.; Rosenau, T.; Van Herwijnen, H.W. Current situation of the challenging scale-up development of hydroxymethylfurfural production. *ChemSusChem* **2020**, *13*, 3544–3564. [\[CrossRef\]](#)
6. Mason, J.B.; Sun, Y. Microwave-Assisted Production of 5-Hydroxymethylfurfural from Glucose. *ChemistrySelect* **2021**, *6*, 10582–10586. [\[CrossRef\]](#)
7. Giovanelli, G.; Cappa, C. 5-hydroxymethylfurfural formation in bread as a function of heat treatment intensity: Correlations with browning indices. *Foods* **2021**, *10*, 417. [\[CrossRef\]](#)
8. Motagamwala, A.H.; Huang, K.; Maravelias, C.T.; Dumesic, J.A. Solvent system for effective near-term production of hydroxymethylfurfural (HMF) with potential for long-term process improvement. *Energy Environ. Sci.* **2019**, *12*, 2212–2222. [\[CrossRef\]](#)
9. Dasthban, M.; Gilbert, A.; Fatehi, P. Recent advancements in the production of hydroxymethylfurfural. *RSC Adv.* **2014**, *4*, 2037–2050. [\[CrossRef\]](#)
10. Slak, J.; Pomeroy, B.; Kostyniuk, A.; Grilc, M.; Likozar, B. A review of bio-refining process intensification in catalytic conversion reactions, separations and purifications of hydroxymethylfurfural (HMF) and furfural. *Chem. Eng. J.* **2022**, *429*, 132325. [\[CrossRef\]](#)
11. Tongtummachat, T.; Akkarawatkhoosith, N.; Jaree, A. Process intensification for 5-hydroxymethylfurfural production from sucrose in a continuous fixed-bed reactor. *Chem. Eng. Res. Des.* **2022**, *182*, 312–323. [\[CrossRef\]](#)
12. Körner, P.; Jung, D.; Kruse, A. The effect of different Brønsted acids on the hydrothermal conversion of fructose to HMF. *Green Chem.* **2018**, *20*, 2231–2241. [\[CrossRef\]](#)
13. Shimizu, K.I.; Uozumi, R.; Satsuma, A. Enhanced production of hydroxymethylfurfural from fructose with solid acid catalysts by simple water removal methods. *Catal. Commun.* **2009**, *10*, 1849–1853. [\[CrossRef\]](#)
14. Hu, Z.; Peng, Y.; Gao, Y.; Qian, Y.; Ying, S.; Yuan, D.; Zhao, D. Direct synthesis of hierarchically porous metal–organic frameworks with high stability and strong Brønsted acidity: The decisive role of hafnium in efficient and selective fructose dehydration. *Chem. Mater.* **2016**, *28*, 2659–2667. [\[CrossRef\]](#)
15. Megías-Sayago, C.; Navarro-Jaén, S.; Drault, F.; Ivanova, S. Recent Advances in the Brønsted/Lewis Acid Catalyzed Conversion of Glucose to HMF and Lactic Acid: Pathways toward Bio-Based Plastics. *Catalysts* **2021**, *11*, 1395. [\[CrossRef\]](#)
16. He, O.; Zhang, Y.; Wang, P.; Liu, L.; Wang, Q.; Yang, N.; Yu, H. Experimental and kinetic study on the production of furfural and HMF from glucose. *Catalysts* **2020**, *11*, 11. [\[CrossRef\]](#)
17. Feng, L.; Wang, K.Y.; Willman, J.; Zhou, H.C. Hierarchy in metal–organic frameworks. *ACS Cent. Sci.* **2020**, *6*, 359–367. [\[CrossRef\]](#)
18. Dissegna, S.; Vervoorts, P.; Hobday, C.L.; Duren, T.; Daisenberger, D.; Smith, A.J.; Kieslich, G. Tuning the mechanical response of metal–organic frameworks by defect engineering. *J. Am. Chem. Soc.* **2018**, *140*, 11581–11584. [\[CrossRef\]](#)
19. Hao, J.; Mao, W.; Ye, G.; Xia, Y.; Wei, C.; Zeng, L.; Zhou, J. Tin–chromium bimetallic metal–organic framework MIL-101 (Cr, Sn) as a catalyst for glucose conversion into HMF. *Biomass Bioenergy* **2022**, *159*, 106395. [\[CrossRef\]](#)
20. Oozeerally, R.; Burnett, D.L.; Chamberlain, T.W.; Walton, R.I.; Degirmenci, V. Exceptionally efficient and recyclable heterogeneous metal–organic framework catalyst for glucose isomerization in water. *ChemCatChem* **2018**, *10*, 706–709. [\[CrossRef\]](#)
21. Burnett, D.L.; Oozeerally, R.; Pertiwi, R.; Chamberlain, T.W.; Cherkasov, N.; Clarkson, G.J.; Walton, R.I. A hydrothermally stable ytterbium metal–organic framework as a bifunctional solid-acid catalyst for glucose conversion. *Chem. Comm.* **2019**, *55*, 11446–11449. [\[CrossRef\]](#) [\[PubMed\]](#)
22. Yabushita, M.; Li, P.; Islamoglu, T.; Kobayashi, H.; Fukuoka, A.; Farha, O.K.; Katz, A. Selective metal–organic framework catalysis of glucose to 5-hydroxymethylfurfural using phosphate-modified NU-1000. *Ind. Eng. Chem. Res.* **2017**, *56*, 7141–7148. [\[CrossRef\]](#)
23. Oozeerally, R.; Ramkhalawan, S.D.; Burnett, D.L.; Tempelman, C.H.; Degirmenci, V. ZIF-8 metal organic framework for the conversion of glucose to fructose and 5-hydroxymethyl furfural. *Catalysts* **2019**, *9*, 812. [\[CrossRef\]](#)
24. Akiyama, G.; Matsuda, R.; Sato, H.; Kitagawa, S. Catalytic glucose isomerization by porous coordination polymers with open metal sites. *Asian J. Chem.* **2014**, *9*, 2772–2777. [\[CrossRef\]](#)
25. Zi, G.; Yan, Z.; Wang, Y.; Chen, Y.; Guo, Y.; Yuan, F.; Wang, J. Catalytic hydrothermal conversion of carboxymethyl cellulose to value-added chemicals over metal–organic framework MIL-53 (Al). *Carbohydr. Polym.* **2015**, *115*, 146–151. [\[CrossRef\]](#) [\[PubMed\]](#)

26. Pertiwi, R.; Oozeerally, R.; Burnett, D.L.; Chamberlain, T.W.; Cherkasov, N.; Walker, M.; Walton, R.I. Replacement of chromium by non-toxic metals in lewis-acid MOFs: Assessment of stability as glucose conversion catalysts. *Catalysts* **2019**, *9*, 437. [[CrossRef](#)]
27. Winarta, J.; Shan, B.; McIntyre, S.M.; Ye, L.; Wang, C.; Liu, J.; Mu, B. A decade of UiO-66 research: A historic review of dynamic structure, synthesis mechanisms, and characterization techniques of an archetypal metal–organic framework. *Cryst. Growth Des.* **2019**, *20*, 1347–1362. [[CrossRef](#)]
28. Zhang, Y.; Li, B.; Wei, Y.; Yan, C.; Meng, M.; Yan, Y. Direct synthesis of metal-organic frameworks catalysts with tunable acid–base strength for glucose dehydration to 5-hydroxymethylfurfural. *J. Taiwan Inst. Chem. Eng.* **2019**, *96*, 93–103. [[CrossRef](#)]
29. Gong, J.; Katz, M.J.; Kerton, F.M. Catalytic conversion of glucose to 5-hydroxymethylfurfural using zirconium-containing metal–organic frameworks using microwave heating. *RSC Adv.* **2018**, *8*, 31618–31627. [[CrossRef](#)]
30. Fu, G.; Cirujano, F.G.; Krajnc, A.; Mali, G.; Henrion, M.; Smolders, S.; De Vos, D.E. Unexpected linker-dependent Brønsted acidity in the (Zr) UiO-66 metal organic framework and application to biomass valorization. *Catal. Sci. Technol.* **2020**, *10*, 4002–4009. [[CrossRef](#)]
31. Oozeerally, R.; Burnett, D.L.; Chamberlain, T.W.; Kashtiban, R.J.; Huband, S.; Walton, R.I.; Degirmenci, V. Systematic modification of UiO-66 metal-organic frameworks for glucose conversion into 5-hydroxymethyl furfural in water. *ChemCatChem* **2021**, *13*, 2517–2529. [[CrossRef](#)]
32. Zhang, Y.; Guan, W.; Song, H.; Wei, Y.; Jin, P.; Li, B.; Yan, Y. Coupled acid and base UiO-66-type MOFs supported on g-C₃N₄ as a bi-functional catalyst for one-pot production of 5-HMF from glucose. *Microporous Mesoporous Mater.* **2020**, *305*, 110328. [[CrossRef](#)]
33. Li, Y.; Meng, X.; Luo, R.; Zhou, H.; Lu, S.; Yu, S.; Lyu, J. Aluminum/Tin-doped UiO-66 as Lewis acid catalysts for enhanced glucose isomerization to fructose. *Appl. Catal. A-Gen.* **2022**, *632*, 118501. [[CrossRef](#)]
34. Zhang, Y.; Zhao, J.; Wang, K.; Gao, L.; Meng, M.; Yan, Y. Green Synthesis of Acid-Base Bifunctional UiO-66 Type Metal-Organic Frameworks Membranes Supported on Polyurethane Foam for Glucose Conversion. *ChemistrySelect* **2018**, *3*, 9378–9387. [[CrossRef](#)]
35. Tangsermvit, V.; Pila, T.; Boekfa, B.; Somjit, V.; Klysubun, W.; Limtrakul, J.; Kongpatpanich, K. Incorporation of Al³⁺ Sites on Brønsted Acid Metal–Organic Frameworks for Glucose-to-Hydroxymethylfurfural Transformation. *Small* **2021**, *17*, 2006541. [[CrossRef](#)] [[PubMed](#)]
36. Lara-Serrano, M.; Morales-delaRosa, S.; Campos-Martin, J.M.; Abdelkader-Fernández, V.K.; Cunha-Silva, L.; Balula, S.S. One-Pot Conversion of Glucose into 5-Hydroxymethylfurfural using MOFs and Brønsted-Acid Tandem Catalysts. *Adv. Sustain. Syst.* **2022**, *6*, 2100444. [[CrossRef](#)]
37. Caratelli, C.; Hajek, J.; Cirujano, F.G.; Waroquier, M.; Xamena, F.X.L.; Van Speybroeck, V. Nature of active sites on UiO-66 and beneficial influence of water in the catalysis of Fischer esterification. *J. Catal.* **2017**, *352*, 401–414. [[CrossRef](#)]
38. Valenzano, L.; Civalieri, B.; Chavan, S.; Bordiga, S.; Nilsen, M.H.; Jakobsen, S.; Lamberti, C. Disclosing the complex structure of UiO-66 metal organic framework: A synergic combination of experiment and theory. *Chem. Mater.* **2011**, *23*, 1700–1718. [[CrossRef](#)]
39. Shearer, G.C.; Chavan, S.; Bordiga, S.; Svelle, S.; Olsbye, U.; Lillerud, K.P. Defect engineering: Tuning the porosity and composition of the metal–organic framework UiO-66 via modulated synthesis. *Chem. Mater.* **2016**, *28*, 3749–3761. [[CrossRef](#)]
40. Feng, X.; Song, Y.; Lin, W. Dimensional Reduction of Lewis Acidic Metal–Organic Frameworks for Multicomponent Reactions. *J. Am. Chem. Soc.* **2021**, *143*, 8184–8192. [[CrossRef](#)]
41. Vo, T.K.; Nguyen, V.C.; Quang, D.T.; Park, B.J.; Kim, J. Formation of structural defects within UiO-66(Zr)-(OH)₂ framework for enhanced CO₂ adsorption using a microwave-assisted continuous-flow tubular reactor. *Microporous Mesoporous Mater.* **2021**, *312*, 110746. [[CrossRef](#)]
42. Li, K.; Du, M.; Ji, P. Multifunctional tin-based heterogeneous catalyst for catalytic conversion of glucose to 5-hydroxymethylfurfural. *ACS Sustain. Chem. Eng.* **2018**, *6*, 5636–5644. [[CrossRef](#)]
43. Chen, J.; Li, K.; Chen, L.; Liu, R.; Huang, X.; Ye, D. Conversion of fructose into 5-hydroxymethylfurfural catalyzed by recyclable sulfonic acid-functionalized metal-organic frameworks. *Green Chem.* **2014**, *16*, 2490–2499. [[CrossRef](#)]
44. Guo, W.; Hensen, E.J.M.; Qi, W. Titanium Phosphate Grafted on Mesoporous SBA-15 Silica as a Solid Acid Catalyst for the Synthesis of 5-Hydroxymethylfurfural from Glucose. *ACS Sustain. Chem. Eng.* **2022**, *10*, 10157–10168. [[CrossRef](#)]
45. Song, X.; Yue, J.; Zhu, Y.; Wen, C.; Chen, L.; Liu, Q.; Wang, C. Efficient Conversion of Glucose to 5-Hydroxymethylfurfural over a Sn-Modified SAPO-34 Zeolite Catalyst. *Ind. Eng. Chem. Res.* **2021**, *60*, 5838–5851. [[CrossRef](#)]
46. Nikolla, E.; Román-Leshkov, Y.; Moliner, M.; Davis, M.E. “One-pot” synthesis of 5-(hydroxymethyl) furfural from carbohydrates using tin-beta zeolite. *ACS Catal.* **2011**, *1*, 408–410. [[CrossRef](#)]
47. Toby, B.H.; Von Dreele, R.B. GSAS-II: The genesis of a modern open-source all purpose crystallography software package. *J. Appl. Crystallogr.* **2013**, *46*, 544–549. [[CrossRef](#)]